

## Population of Rydberg states by electron capture in fast-ion—atom collisions

J. Burgdörfer\*

*Institut für Atom- und Festkörperphysik, Freie Universität, Arnimallee 14, 1000 Berlin 33, West Germany*

L. J. Dubé

*Fakultät für Physik, Universität Freiburg, Hermann-Herder-Strasse 3, 7800 Freiburg, West Germany*

(Received 29 August 1984)

The  $l, m$ -substate distribution in low-lying Rydberg manifolds ( $n \approx 10$ ) following electron capture  $H^+ + H(1s) \rightarrow H(n) + H^+$  is calculated at high velocities ( $v > 1$  a.u.) in the continuum-distorted-wave (CDW) approximation. The standard CDW approximation is modified to account for final-state Stark mixing of the Rydberg manifold in the exit channel using the post-collision-interaction model. The influence of multiple-scattering contributions is analyzed and comparison is made with  $\sigma_{lm}$  predicted by the Born approximation. We find that the double-scattering contribution, closely connected with the classical Thomas process, becomes visible in the CDW approximation at surprisingly low nonasymptotic velocities.

### I. INTRODUCTION

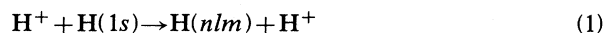
The formation of Rydberg states in ion-atom and ion-solid collisions has gained considerable interest in recent years. From an experimental point of view this interest is largely motivated by the observation that a considerable fraction of the projectiles leave the target in highly excited states<sup>1-4</sup> and that these weakly bound electrons can be strongly affected by even weak (laboratory) electric and magnetic fields.<sup>5,6</sup> The theoretical study has been stimulated by Shakeshaft and Spruch, who pointed out, in a series of papers,<sup>7-9</sup> that capture into Rydberg states provides a possibility to isolate second-order Born effects in the charge-transfer process.

It is now widely believed (although not proven) that at asymptotically high velocities  $v \gg v_{p,T}$  (with  $v_p = Z_p/n$  and  $v_T = Z_T/n'$  being the orbital velocities of the electron in the projectile and target state, respectively) the second-order Born term provides the leading contribution to the cross section. The second Born (B2) amplitude is intimately connected with the classical double-scattering process originally proposed by Thomas<sup>10</sup> which describes electron capture as a sequence of two binary collisions: a quasifree electron is first scattered off the projectile through an angle of  $60^\circ$  with respect to the projectile velocity  $\vec{v}$  and then scattered through  $60^\circ$  off the target in such a way as to leave the electron with almost zero velocity in the rest frame of the projectile. The quantum-mechanical double scattering process as described by the second term in a Born expansion is thought to dominate at asymptotically high velocities because of its uniform velocity dependence  $\propto v^{-11}$  irrespective of the initial and final states involved. This contrasts with the faster falloff in the first Born approximation (usually referred to as the Oppenheimer-Brinkman-Kramers (OBK) approximation)  $\sigma \propto v^{-12-2l-2l'}$  with a strong dependence on the angular momenta of the initial ( $l'$ ) and final ( $l$ ) states. The single-scattering process described by the OBK approximation is an intrinsic quantum-mechanical process. Since

capture of a free electron in a single binary collision is classically forbidden the charge transfer is mediated only by the high-momentum components of the bound-state wave functions, or equivalently in coordinate space, by the portion of the wave function at small distances from the nucleus.

The asymptotic regime where the B2 analysis is expected to be valid can be reached at moderate laboratory velocities ( $v \approx 1$  a.u.) only for Rydberg-to-Rydberg charge transfer<sup>9,11</sup> (or in a somewhat related process in ion-molecule scattering<sup>12</sup>) where both orbital velocities are small;  $v_{p,T} \ll 1$ . For processes involving ground-state-to-ground-state capture, however, the asymptotic regime is not reached unless the projectile energy exceeds several MeV/nucleon. First evidence of the Thomas peak in the differential capture cross section has recently been found<sup>13</sup> for  $H^+ + He$  at 7.4 MeV ( $v \approx 17.2$  a.u.).

We consider in the following the ground- to Rydberg-state charge-transfer process for the symmetric system ( $Z_p = Z_T$ ),



at intermediate velocities  $v \geq 1$  where the asymptotic regime has been reached with respect to the final state ( $v \gg v_p$ ) but not with respect to the target state and where experimental investigations are most likely to be feasible. We confine ourselves in this communication to "low" Rydberg states ( $n \approx 10$ ) relying on the fact that for  $n \gg 1$  (or, more precisely,  $n \gg Z_p/v$ ) cross sections are only weakly dependent on the principal quantum number  $n$  except for a common scaling factor  $\sim n^{-3}$ .

Previous results obtained with the exact<sup>14</sup> or the peaking<sup>11</sup> B2 approximation do not provide a reliable estimate of the capture cross sections at finite velocities. The only available exact B2 calculation for  $1s \rightarrow 1s$  charge transfer<sup>14</sup> has shown to fail completely at moderate velocities (in this energy region  $\sigma_{B2} > \sigma_{OBK}$  where the latter already overestimates the experimental data) pointing out

the slow convergence of a Born-type perturbation expansion. Furthermore, the additional peaking approximation is in strong disagreement with the exact result except for asymptotic velocities.

Several multiple-scattering approaches including higher-order contributions have now been devised<sup>15</sup> to remedy this situation. We employ in our study a multiple scattering approach, the continuum-distorted wave (CDW) approximation.<sup>16</sup> Despite several deficiencies discussed by Taulbjerg,<sup>17</sup> the CDW has some major advantages:

(i) It treats distortion of the entrance and exit channel on equal footing and therefore is well suited for nearly symmetric collision systems.

(ii) It gives reasonable agreement with experimental data for integrated cross sections.

(iii) The capture amplitude is available in analytic form for arbitrary final states.<sup>18,19</sup> By comparing with corresponding results for the population of Rydberg levels in first and second Born approximations (in peaking approximation) we will study the influence of various higher-order contributions over a wide range of final-state quantum numbers.

In our investigation of Rydberg states special attention has to be paid to the influence of long-range Stark mixing in the exit channel. Hydrogenic manifolds with a large number of different angular momentum states are extremely sensitive to final-state interactions with the residual target ion. We incorporate Stark mixing within a modified CDW approximation, the CDW-PCI approximation in a nonperturbative albeit approximative form with the help of the post collision interaction (PCI) model.<sup>20</sup> This allows a detailed analysis of the influence of angular momentum mixing by an electric field in Rydberg states. Atomic units are used throughout.

## II. THEORY

For the sake of clarity we briefly review the major steps of our theoretical approach. A more detailed discussion can be found elsewhere.<sup>19-23</sup>

The cross section integrated over all scattering angles of the projectile for capture into a hydrogenic  $nlm$  state is given by

$$\sigma_{nlm} = \frac{1}{(2\pi)^2 v} \int d^3k |t_{nlm}(\vec{k})|^2 \delta(\vec{k} \cdot \vec{v} + v^2/2 + \Delta\epsilon), \quad (2)$$

where  $t_{nlm}(\vec{k})$  denotes the transition matrix element from a  $1s$  initial state to a final  $nlm$  state as a function of the momentum transfer  $\vec{k}$  with  $\Delta\epsilon = \epsilon_f - \epsilon_i$  being the resonance defect. The quantization axis is chosen to coincide with the direction of the projectile velocity ( $\hat{v} = \hat{z}$ ).

The transition amplitude in the CDW approximation<sup>16</sup> can be evaluated most conveniently by expanding (2) in terms of parabolic states<sup>18,19</sup>

$$t_{nlm}^{\text{CDW}}(\vec{k}) = \sum_{n_1=0}^{n-|m|-1} C_{n_1}(n, l, m) t_{n_1 n_2 m}^{\text{CDW}}(\vec{k}) \quad (3)$$

with

$$C_{n_1}(n, l, m) = (-1)^{n_1 + (|m| - m)/2} \sqrt{2l+1} \times \begin{pmatrix} \frac{n-1}{2} & \frac{n-1}{2} & l \\ |m| + n_2 - n_1 & |m| - n_2 + n_1 & -|m| \end{pmatrix} \quad (4a)$$

and

$$n = n_1 + n_2 + |m| + 1 \quad (4b)$$

according to the unitary  $O(4)$  transformation between the different representations of the hydrogenic wave functions. The representation of the transition operator in the parabolic basis is particularly convenient for incorporating final-state Stark mixing. The long-range Coulomb interaction between the excited electron and the residual target ion leads to a strong mixing of the degenerate  $l$  states within a Rydberg manifold: this occurs at large internuclear separations long after the primary charge transfer has taken place. This process can be treated analytically in a nonperturbative but still approximate way, through the post-collision-interaction (PCI) model.<sup>20</sup> Restricting to the leading dipole term in a multipole expansion of the electron-target interaction the evolution operator is given by

$$U^{\text{PCI}}(\infty, R_0) \cong \exp \left[ (i/v) \int_{R_0}^{\infty} dR \vec{F}(R) \cdot \vec{d} \right], \quad (5)$$

where  $\vec{F}(R) = (Z_T'/R^2)\hat{z}$  is the electric field of the target ion at large distances and  $\vec{d} = -\vec{r}$  the dipole operator. The lower limit of the phase integral is chosen as the smallest radius within the given manifold, namely,  $R_0 = \langle r \rangle_{n, l=n-1} = (2n^2 + n)/2Z_P$ . In Eq. (5) we allow for the asymptotic charge  $Z_T'$  seen by the electron at large distances to be different from the full nuclear charge  $Z_T$  for nonhydrogenic targets. In the present case we have obviously  $Z_T = Z_T' = 1$  and no ambiguity occurs.

The evolution operator [Eq. (5)] is diagonal in the parabolic basis. Consequently, the modified CDW amplitude  $t_{nlm}^{\text{CDW-PCI}}$  taking into account final-state Stark mixing is given by

$$t_{n_1 n_2 m}^{\text{CDW-PCI}}(\vec{k}) = e^{i\phi_{n_1 n_2 m}} t_{n_1 n_2 m}^{\text{CDW}}(\vec{k}) \quad (6)$$

with the Stark phase

$$\phi_{n_1 n_2 m} = \frac{3}{v} \frac{Z_T' n(n_2 - n_1)}{2R_0 Z_P}. \quad (7)$$

Concurrently with our CDW calculation we have performed a similar calculation with the modified OBK approximation,

$$t_{n_1 n_2 m}^{\text{OBK-PCI}}(\vec{k}) = e^{i\phi_{n_1 n_2 m}} t_{n_1 n_2 m}^{\text{OBK}}(\vec{k}), \quad (8)$$

where  $t_{nlm}^{\text{OBK}}$  denotes the standard OBK transition amplitude.<sup>8</sup>

Comparing the perturbation expansion for the CDW transition amplitude with the Born series for charge transfer

$$t_{nlm}(\vec{k}) = t_{nlm}^{(1)}(\vec{k}) + t_{nlm}^{(2)}(\vec{k}) + t_{nlm}^{(3)}(\vec{k}) + \dots \quad (9)$$

one arrives at<sup>23</sup>

$$t_{nlm}^{\text{CDW}}(\vec{k}) = t_{nlm}^{(1)}(\vec{k}) + t_{nlm}^{(2)'}(\vec{k}) + t_{nlm}^{(3)'}(\vec{k}) + \dots, \quad (10)$$

where  $t^{(n)}$  denotes the  $n$ th order term in the perturbation expansion. Correspondingly, the first- and second-order Born approximations are given by

$$t_{nlm}^{\text{OBK}}(\vec{k}) = t_{nlm}^{(1)}(\vec{k}) \quad (11)$$

and

$$t_{nlm}^{\text{B2}}(\vec{k}) = t_{nlm}^{(1)}(\vec{k}) + t_{nlm}^{(2)}(\vec{k}), \quad (12)$$

respectively. The primes in (10) indicate that all higher-order terms ( $n \geq 2$ ) in the CDW amplitude are incomplete with respect to the corresponding full Born series [Eq. (9)]. The incompleteness of the double-scattering term  $t_{nlm}^{(2)'}$  in the CDW approximation has recently become evident in the dip in the differential cross section at the Thomas peak<sup>24</sup> and in the deviations in the asymptotic  $v^{-11}$  coefficient in the integrated cross section for non- $s$  states.<sup>19</sup> This deficiency will become particularly important for capture into states with large  $l$ . Despite this difficulty the merits of the CDW approximation lie in the partial inclusion of triple- and higher-order scattering contributions ( $n \geq 3$ ); at finite velocities, these multiple-scattering contributions are responsible for bringing the theoretical cross sections and experimental data in closer agreement. Similarly, the PCI correction incorporates higher-order terms which are effective in intrashell mixing. The PCI introduces corrections of order  $(Z_T/v)$  thus leaving unaltered the asymptotically leading  $v^{-11}$  term in the cross section.

### III. RESULTS AND DISCUSSION

In Figs. 1 and 2 we present the  $lm$  distributions  $\sigma_{lm}$  in  $n=10$  for the capture process [Eq. (1)] at  $v=1$  a.u. calculated in the OBK, OBK-PCI, CDW, and CDW-PCI approximations. Only positive  $m$  values are shown in view of the symmetry relation  $\sigma_{lm} = \sigma_{l-m}$ . Although these calculations have been performed at the matching velocity ( $v=v_T$ ) and therefore should be taken with some caution, the dramatic effect of multiple-scattering contributions is clearly visible. For large angular momenta the CDW cross sections are several orders of magnitude larger than those in the OBK approximation. Moreover the relative  $lm$  distribution is entirely different. The OBK distributions fall off monotonically with increasing  $l$  and  $m$ : this is caused by the reduction of the high-momentum components, or equivalently, by the reduction of the amplitude of the wave function near the nucleus with increasing angular momenta. The sensitivity to momentum matching implies also a strong directional anisotropy: orbits with high  $m$  lying in a plane perpendicular to  $\vec{v}$  maximize the momentum mismatch and, consequently, have exceedingly small cross sections. The OBK approximation leads to a highly aligned Rydberg manifold. The CDW approximation, on the other hand, shows an "oscillatory" behavior of  $\sigma_{lm}$  for (fixed) large  $l$ . A similar trend has

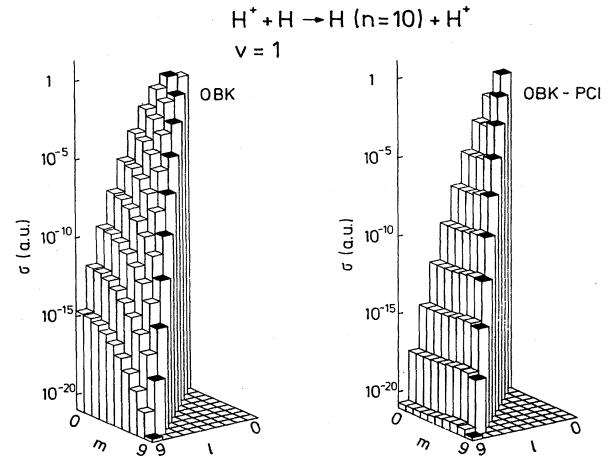


FIG. 1.  $\sigma_{lm}$  (a.u.) for  $H^+ + H(1s) \rightarrow H(n=10) + H^+$  at  $v=1$  a.u. in OBK and OBK-PCI approximations. The maxima of the cross section along the  $l$  axis for a fixed value of  $m$  are marked.

been observed previously by Crothers and McCann<sup>18</sup> in their study of the asymmetric system,  $C^{6+} \rightarrow H$ , but an explanation of the oscillatory structure has remained an open question. As we will show below, the  $m$  oscillations are related to the presence of the double scattering term,  $t^{(2)'}$ , which is expected in analogy with the B2 approximation to provide the dominant contribution to the full scattering amplitude at high velocities.

Figure 1 and 2 reveal also some spectacular changes of the  $lm$  distribution caused by post collisional Stark mixing. The PCI induces a probability flux along the  $l$  axis with  $\Delta m=0$  from higher to lower  $l$  values. In effect, the alignment of the primary OBK distribution is almost completely removed (Fig. 1). A different picture emerges from the CDW-PCI model (Fig. 2). The PCI effect is generally less pronounced and in some cases tends to increase the nonstatistical population by enhancing the  $m$

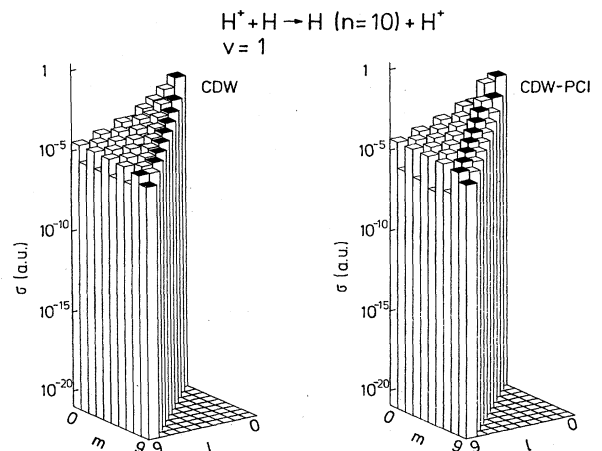


FIG. 2.  $\sigma_{lm}$  (a.u.) for  $H^+ + H(1s) \rightarrow H(n=10) + H^+$  at  $v=1$  a.u. in CDW and CDW-PCI approximations. The maxima of the cross section along the  $l$  axis for a fixed value of  $m$  are marked.

oscillations. The changes in the  $\sigma_{lm}$  distribution at  $v=2$  a.u. are shown in more detail in Fig. 3. The redistribution to lower  $l$  values by the PCI can clearly be seen, in particular along the line  $(l=3, m=0) \rightarrow (2,0) \rightarrow (1,0) \rightarrow (0,0)$ . Furthermore, the local minima at  $l=9$ ;  $m=1,3$ , and  $5$  become more pronounced due to the coupling to neighboring  $l=8$  states with the same azimuthal quantum number.

Although a detailed analysis of PCI effects requires in general the knowledge of the complete density matrix of an  $n$  manifold<sup>22</sup> (including the offdiagonal coherence matrix elements entering the present calculation) a few general trends may be readily extracted as follows: At high velocities the sign of the coherence matrix elements in the OBK and CDW approximations are such that the flux is directed towards lower angular momenta in the case of an attractive final-state interaction. We remark parenthetically that a repulsive image-force on the electron of a highly charged ion near metal surfaces would favor a probability flux in the opposite direction to higher  $l$  values. This could have some relevance in studies of Rydberg states formed in beam-foil interaction.<sup>4</sup> The PCI effects are reduced with increasing projectile velocities because of the shorter interaction times  $\sim 1/v$  in the field. The PCI mixing is enhanced at low  $m$  values because the mixing angle given by the Stark phase  $\phi_{n_1 n_2 m}$  increases as  $m$  decreases [Eqs. (4b) and (7)]. Finally, the PCI couples predominantly neighboring states  $(l, m \leftrightarrow l \pm 1, m)$  corresponding to optically allowed transitions. The redistribution is therefore most effective whenever the primary cross section distribution provides a large "gradient" along the  $l$  axis; i.e., large population differences between neighboring states. Remark that these qualitative features are independent of the actual choice of the lower limit in the phase integral [Eq. (7)].

Let us now return to a more detailed analysis of the oscillatory structures in the CDW distributions. We observe that the (almost) regular oscillations at  $v=1$  (Fig. 2) have evolved for  $l \geq 5$  into an irregular oscillation pattern at  $v=2$  (Fig. 3). Further calculations at higher velocities reveal that this pattern develops into a converged structure, as, for example, shown in Fig. 4 for  $v=20$ . The persistence of this oscillatory behavior as  $v$  is further increased suggests that an explanation of the oscillations in the  $m$  distributions (for fixed  $l$ ) may be obtained by exam-

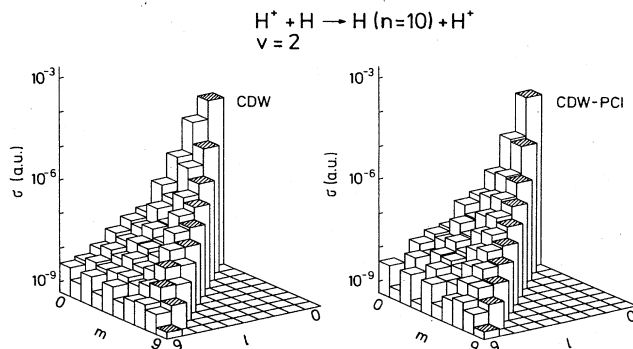


FIG. 3.  $\sigma_{lm}$  (a.u.) for  $H+H(1s) \rightarrow H(n=10)+H^+$  at  $v=2$  a.u. in CDW and CDW-PCI approximations.

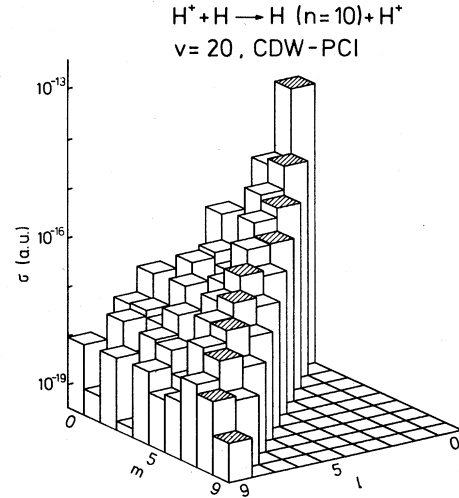


FIG. 4.  $\sigma_{lm}$  (a.u.) following electron capture  $H^+ + H(1s) \rightarrow H(n=10) + H^+$  in CDW-PCI approximation at  $v=20$  a.u.

ining the predictions of the asymptotic B2 approximation. This idea is substantiated by the observation that the double scattering term (such as  $t^{(2)}$ , for CDW) of a number of multiple scattering approaches has been shown<sup>25</sup> to give rise to the dominant contribution to the asymptotic cross section.

This conjecture is confirmed by comparing the OBK and CDW distributions with the relative  $lm$  cross sections predicted by the B2 approximation<sup>7</sup> at asymptotically high velocity

$$\sigma_{lm}^{B2} \propto |Y_{lm}(\theta=60^\circ, \varphi)|^2. \quad (13)$$

This simple dependence on the quantum numbers  $l$  and  $m$  originates solely, as  $v \rightarrow \infty$ , from the double-scattering term,  $t^{(2)}$ , and is identical with that predicted by the classical Thomas scattering. For more details we refer the reader to Ref. 7 and 8. The comparison of  $\sigma_{lm}^{B2}$  with the OBK and CDW cross sections (without PCI) is presented in Fig. 5 for the  $n=7$  manifold and for velocities ranging from  $v=1$  to 6. The evolution of  $\sigma_{lm}^{CDW}$  into the Thomas scattering distribution is clearly observed: the larger the  $l$  value concerned, the faster the convergence. One notices also that the onset of this development appears at surprisingly low velocities, just above the target matching velocity. This contrasts strongly with the predictions of the B2 approximation<sup>8,11</sup> where the velocities necessary to reach the limiting distribution (13) are appreciably larger. In other words, in the velocity range presented in Fig. 5 the single-scattering term,  $t^{OBK}$ , still dominates over the double-scattering term,  $t^{(2)}$ .

Insight into the relative importance of different terms in the CDW amplitude [Eq. (10)] may also be obtained by a look at the OBK distributions (shown in Fig. 5 only in cases where the cross sections are of comparable magnitude). For lower  $l$  and  $m$  where momentum mismatch is not too severe,  $\sigma_{lm}^{OBK}$  exceed  $\sigma_{lm}^{CDW}$  at all velocities considered. One expects this reduction to be due to the interference between  $t^{(3)}$ , (and higher order) and  $t^{(1)}$  such as

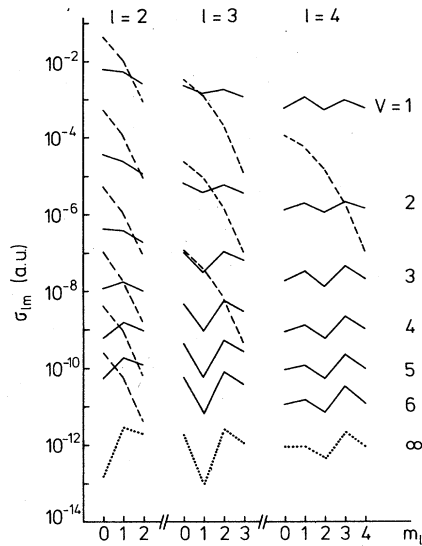


FIG. 5.  $\sigma_{lm}$  ( $l=2,3,4$ ) following electron capture  $H^+ + H(1s) \rightarrow H(n=7) + H^+$  at different velocities  $v=1-6$  a.u.; --- OBK; — CDW;  $\cdots$  asymptotic  $lm$  distribution  $\sigma_{lm}^{B2} \propto |Y_l^m(\theta_T)|^2$  (arbitrarily scaled). Only a few OBK cross sections are plotted; all others are small compared with the CDW results.

to enhance the relative importance of  $t^{(2)}$ , and thereby to promote the appearance of the Thomas scattering distribution even at moderate velocities (e.g., above  $v=3$  for  $l=2$ ). For higher  $l$ , and  $m$ , the amplitudes  $t^{(2)}$ ,  $t^{(3)}$ , ... are entirely responsible for the magnitude of  $\sigma_{lm}^{CDW}$  since  $\sigma_{lm}^{OBK}$  is already negligibly small at  $v=1$ . The fast convergence of  $\sigma_{lm}^{CDW}$  to the Thomas scattering distribution is

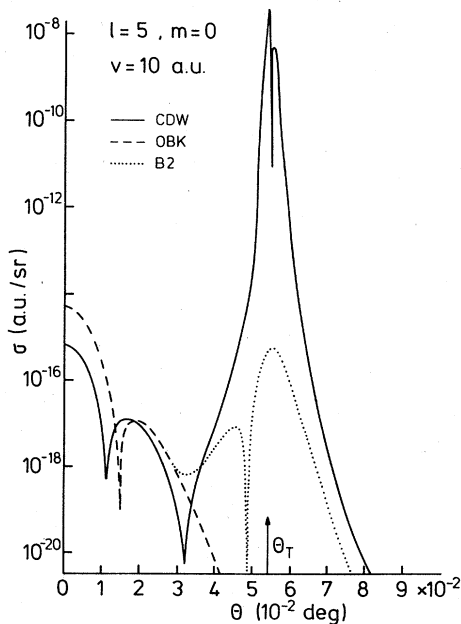


FIG. 6. Differential cross section  $\sigma_{nlm}(\theta)$  for  $H^+ + H(1s) \rightarrow H(n=7, l=5, m=0) + H^+$  at  $v=10$  a.u. as a function of the center-of-mass scattering angle  $\theta$ . --- OBK; — CDW;  $\cdots$  (peaking) B2.

a clear indication, however, of the rapid dominance of  $t^{(2)}$ , over all other multiple scattering terms.

Further evidence for the importance of the double scattering term can be found in the differential capture cross section

$$\sigma_{nlm}(\theta) = \frac{\mu^2}{(2\pi)^2} |t_{nlm}(\vec{k})|^2 \quad (14)$$

[ $k_z = -(\Delta\epsilon + v^2/2)/v$ ,  $k_x = \mu\theta v$ ;  $\mu$  denotes the reduced mass] shown in Fig. 6 for  $n=7$ ,  $l=5$ , and  $m=0$  at  $v=10$  a.u. A unique signature of the double-scattering contribution is the peak in  $\sigma_{nlm}(\theta)$  at the characteristic Thomas angle  $\theta_T = 0.054^\circ$  in the center-of-mass frame. The OBK approximation shows a second peak at zero degree. In the second Born approximation (with peaking approximation) the two peaks due to  $t^{(1)}$  and  $t^{(2)}$  give contributions of comparable magnitude to the integrated cross section. By contrast, a strong enhancement of the Thomas peak relative to the  $t^{(1)}$  peak and, in addition, a narrow dip precisely at the top of the Thomas peak can be observed in the CDW approximation.

To complete the picture of the relative importance of the single and multiple scattering contributions to the CDW amplitude we examine next the velocity dependence of the subshell cross section

$$\sigma_l \equiv \sum_m \sigma_{lm} \quad (15)$$

The results are displayed in Fig. 7. For the  $s$  state the (destructive) interference between the single- and the multiple-scattering terms reduces  $\sigma_{l=0}^{CDW-PCI}$  to values below  $\sigma_{l=0}^{OBK-PCI}$  over the whole range of velocities. With increasing  $l$  quantum numbers, the  $\sigma_l^{CDW-PCI}$  and  $\sigma_l^{OBK-PCI}$  curves cross each other at decreasing velocities. These crossing points lie for the  $p$  state at  $v \approx 10$ , for the  $d$

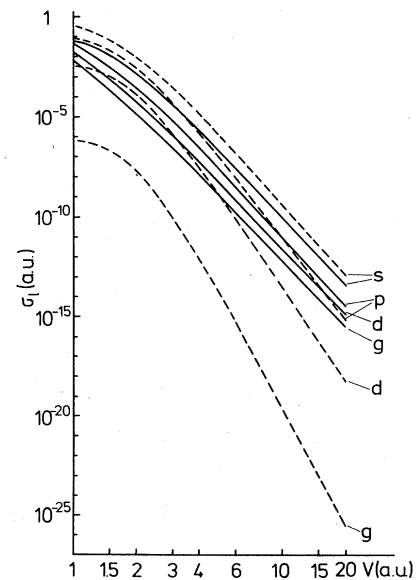


FIG. 7. Velocity dependence of subshell cross sections  $\sigma_l$  following  $H^+ + H(1s) \rightarrow H(n=7) + H^+$ ; --- OBK-PCI; — CDW-PCI.

state at  $v \sim 3.2$  and already for the  $f, g, \dots$  states is  $\sigma_{l \geq 3}^{\text{OBK-PCI}} < \sigma_{l \geq 3}^{\text{CDW-PCI}}$  for  $v \geq 1$ .

As mentioned earlier, it is important to realize that the velocities at which higher-order terms (in particular,  $t^{(2)'}$ ) included in the CDW approximation start to dominate lie considerably lower than previous estimates obtained from the B2 approximation.<sup>8,11</sup> A major cause of these features in the differential and integrated cross section may be attributed to the incorrect form of  $t^{(2)'}$ . Indeed we find it to give asymptotic  $v^{-11}$  coefficients which for all non- $s$  states overestimate the correct double-scattering contribution. The correction factors<sup>19</sup> are  $R_{2p}(v \rightarrow \infty) \equiv \sigma_{2p}^{\text{CDW}} / \sigma_{2p}^{\text{B2}} = 3$ ,  $R_{3d}(v \rightarrow \infty) = 32$ . Numerical results indicate further that  $R_{nl}(v \rightarrow \infty)$  is weakly dependent on  $n$  but rapidly increasing with  $l$ . For example, at  $v = 50$ , one has  $R_{7p} = 3.95$ ,  $R_{7d} = 29.35$ ,  $R_{7f} = 286.7$ ,  $R_{7g} = 3.766 \times 10^4$ , etc. We therefore expect the incorrect double-scattering contribution to magnify the cross sections especially near the Thomas peak also at lower velocities. Clearly more theoretical work is needed to develop a multiple scattering approach containing the complete double-scattering amplitude and which would merge with the B2 approximation at high velocities. The impulse approximation<sup>26</sup> and the strong potential Born approximation<sup>27</sup> valid for asymmetric systems belong to this category but implementation over a large range of quantum numbers is still lacking.

#### IV. CONCLUDING REMARKS

In the present exploratory study, we have examined the population of Rydberg states produced by electron capture in a symmetric collision system. The theoretical treatment based on a single-scattering approach (OBK) and a multiple-scattering method (CDW) has attempted to isolate two distinct effects, namely, the influence (i) of the post collisional Stark interaction, and (ii) of the inclusion of multiple scattering contributions on a description of the final-state distributions.

Our findings are as follows. The post collisional Stark interaction which we introduce analytically (although approximately) to modify the primary capture amplitude, leads to dramatic changes in the substate cross sections within a Rydberg manifold. The Stark mixing due to the residual electric field of the target induces a shift of the capture probability to lower  $l$  values. The OBK and CDW approximations respond differently to the Stark

mixing, the effects being more pronounced in the first-order theory. Also since the residence time of the projectile in the interaction region is  $\propto 1/v$ , these effects decrease with increasing projectile velocity. For capture into high  $l$  states, the CDW cross sections are orders of magnitude larger than those of the OBK approximation. This indicates the importance of higher-order terms in mediating the electron transfer into large  $l$  values. Moreover, the signature of the double-scattering term shows up in the CDW approximation in a magnetic substate population which rapidly converges to a substate distribution  $\propto |Y_{lm}(\theta = 60^\circ, \varphi)|^2$  in accord with the Thomas scattering (or equivalently the asymptotic B2) distribution. The onset of this convergence, however, happens at remarkably low velocities and appears to be an intrinsic property of the CDW Ansatz, due, in particular, to the specific form of the double-scattering term incorporated (implicitly) in the approximation.

These results suggest an experimental investigation of the magnetic substate population as a sensitive testing ground for charge transfer theories. Several possibilities may be considered: for low  $n$  values the substate distribution may be extracted from a polarization experiment. In this case a non-hydrogenic projectile may be more favorable to achieve sufficient spectral resolution in order to sort out the different angular momentum components. This, in turn, would introduce some ambiguities in comparing with theory. Alternatively, microwave resonance techniques<sup>28</sup> have recently proven to be very successful in determining substate cross sections. For higher  $n$  values recent progress in field-ionization<sup>5,29</sup> may facilitate an extraction of the spatial anisotropies in high Rydberg states. This would require an extension of the theoretical analysis to much higher  $n$  (and  $l$ ) values ( $n \geq 30$ ) where field ionization can be expected to be most efficient.

Finally we point out that conclusions are not restricted to symmetric collision partners ( $Z_p \sim Z_T$ ) but also apply to asymmetric systems ( $Z_p > Z_T$ ). In view of the feasibility of observation<sup>30</sup> of charge transfer from Rydberg-to-Rydberg state, we expect in subsequent work to eliminate the restriction of an initial ground state to consider capture from an arbitrary excited state.

#### ACKNOWLEDGMENT

This work was supported in part by the Sonderforschungsbereich 161 of the Deutsche Forschungsgemeinschaft.

\*Permanent address: Department of Physics, University of Tennessee, Knoxville, TN 37996.

<sup>1</sup>K. Berkner, S. Kaplan, G. Paulikas, and R. Pyle, Phys. Rev. **138**, A410 (1965).

<sup>2</sup>P. Hvelplund, H. Haugen, H. Knudsen, L. Andersen, H. Damsgaard, and F. Fukasawa, Phys. Scr. **24**, 40 (1981); S. Datz, in *Atomic Physics 8*, edited by I. Lindgren, A. Rosén, and S. Svanberg (Plenum, New York, 1983), p. 369.

<sup>3</sup>R. Bruch, L. J. Dubé, E. Träbert, P. Heckmann, B. Raith, and K. Brand, J. Phys. B **15**, L857 (1982).

<sup>4</sup>H.-D. Betz, D. Rösenthaler, and J. Rothermel, Phys. Rev. Lett. **50**, 34 (1983).

<sup>5</sup>P. Koch and D. Mariani, Phys. Rev. Lett. **46**, 1275 (1981).

<sup>6</sup>R. H. Garstang, Rep. Prog. Phys. **40**, 105 (1977); J. Castro, M. Zimmerman, R. Hulet, and D. Kleppner, Phys. Rev. Lett. **45**, 1780 (1980).

<sup>7</sup>R. Shakeshaft, Phys. Rev. A **10**, 1906 (1974).

<sup>8</sup>R. Shakeshaft and L. Spruch, J. Phys. B **11**, L457 (1978); Rev. Mod. Phys. **51**, 369 (1979).

<sup>9</sup>L. Spruch, Phys. Rev. A **18**, 2016 (1978).

- <sup>10</sup>L. H. Thomas, Proc. R. Soc. A **114**, 561 (1927).
- <sup>11</sup>J. S. Briggs and L. J. Dubé, J. Phys. B **13**, 771 (1980); L. J. Dubé and J. S. Briggs, *ibid.* **14**, 4595 (1981).
- <sup>12</sup>M. Breinig, G. J. Dixon, P. Engar, S. B. Elston, and I. A. Sellin, Phys. Rev. Lett. **51**, 1251 (1983).
- <sup>13</sup>E. H. Horsdal-Pedersen, C. L. Cocke, and M. Stöckli, Phys. Rev. Lett. **50**, 1910 (1983).
- <sup>14</sup>P. R. Simony and J. H. McGuire, J. Phys. B **14**, L737 (1981); P. R. Simony, Ph.D. thesis, Kansas State University, 1981 (unpublished); J. H. McGuire, P. R. Simony, O. L. Weaver, and J. Macek, Phys. Rev. A **26**, 1109 (1982).
- <sup>15</sup>J. Briggs, K. Taulbjerg, and J. Macek, Comments At. Mol. Phys. **12**, 1 (1982).
- <sup>16</sup>I. M. Cheshire, Proc. Phys. Soc. (London) **84**, 89 (1964).
- <sup>17</sup>K. Taulbjerg, in *Fundamental Processes in Energetic Atomic Collisions*, edited by H. O. Lutz, J. S. Briggs, and H. Kleinpoppen (NATO-ASI series, Plenum, New York, 1983), p. 349.
- <sup>18</sup>D. S. F. Crothers and J. F. McCann, Phys. Lett. **92A**, 170 (1982); Dz. Belkić, R. Gayet, and A. Salin, Comput. Phys. Commun. **30**, 193 (1983).
- <sup>19</sup>L. J. Dubé, J. Phys. B **17**, 641 (1984).
- <sup>20</sup>J. Burgdörfer, Phys. Rev. A **24**, 1756 (1981).
- <sup>21</sup>J. Burgdörfer and L. J. Dubé, Phys. Rev. Lett. **52**, 2225 (1984).
- <sup>22</sup>L. J. Dubé and J. Burgdörfer (unpublished).
- <sup>23</sup>J. Burgdörfer (unpublished).
- <sup>24</sup>R. Rivarola and J. Miraglia, J. Phys. B **15**, 2221 (1982); D. S. F. Crothers and J. F. McCann, *ibid.* **17**, L177 (1984).
- <sup>25</sup>L. J. Dubé, J. Phys. B **16**, 1783 (1983).
- <sup>26</sup>T. Pradhan, Phys. Rev. **105**, 1250 (1957); M. R. C. McDowell, Proc. R. Soc. A **264**, 277 (1961).
- <sup>27</sup>H. Macek and K. Taulbjerg, Phys. Rev. Lett. **46**, 170 (1981); J. H. Macek and S. Alston, Phys. Rev. A **26**, 250 (1982).
- <sup>28</sup>R. J. Knize, S. R. Lundeen, and F. M. Pipkin, Phys. Rev. A **29**, 1114 (1984).
- <sup>29</sup>Z. Vager, E. P. Kanter, D. Schneider, and D. S. Gemmell, Phys. Rev. Lett. **50**, 954 (1983).
- <sup>30</sup>R. G. Rolfes and K. B. MacAdam, J. Phys. B **15**, 4591 (1982).